Prediction of Solar Radiation using Deep LSTM-based Machine Learning Algorithm

K. C. Jayasankar[1], G. Anandhakumar[1]* and A. Kalaimurugan[2]
[1]Department of Electrical and Electronics Engineering, Saveetha School of Engineering, SIMATS, Saveetha University, Chennai, TN, India
[2]Department of Electrical and Electronics Engineering, Agni College of Technology, Chennai, TN, India
Received: 29.04.2024   Accepted: 24.06.2024   Published: 30.09.2024
*anandhakumar@saveetha.com
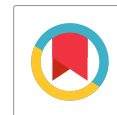
ABSTRACT

Solar radiation, a critical parameter for various applications such as solar energy systems and weather forecasting, exhibits complex temporal patterns influenced by numerous environmental factors. In the quest to enhance the accuracy of solar radiation predictions, this study introduces a novel approach utilizing Deep Long Short-Term Memory (Deep LSTM) networks, a type of recurrent neural network (RNN) known for its capability to model sequential data. Traditional prediction methods often struggle to capture these intricacies, leading to sub-optimal performance. This investigation is based on a Deep LSTM-based machine learning algorithm designed to predict solar radiation with elevated exactitude. The model is meticulously trained on copious datasets encompassing historical meteorological data, including temperature, humidity, wind velocity, and antecedent solar radiation metrics. Pivotal stages encompass data preprocessing, judicious feature selection, and hyperparameter optimization to enhance the model's predictive efficacy. Empirical results clearly illustrate that the Deep LSTM model surpasses traditional methodologies, attaining superior accuracy and resilience across diverse meteorological scenarios. The ramifications of this endeavor portend significant advancements in the strategic planning and administration of solar energy resources, thereby contributing to more dependable and efficacious renewable energy systems.

Keywords: Long short-term memory; Switched reluctance circular motion of structure arms; Learning rate; Accuracy; Deep LSTM; RMSE; ANN; Fuzzy Logic; Convolutional Neural Network.

1. INTRODUCTION

Forecasting solar irradiance stands as a pivotal facet in the efficient operation and governance of solar energy infrastructures. Precise prognostication of solar irradiance holds the potential to significantly enhance the efficacy of solar power installations, streamline grid integration processes, and elevate the dependability of solar energy setups. Within this discourse, the authors introduced a methodology aimed at predicting hourly solar irradiance over short-to-medium durations. This methodology amalgamates insights into cloud coverage levels and historical solar irradiance records, thereby amplifying the efficacy and precision of the predictive model (Bao *et al*. 2017). Research indicates that predictive models employing Artificial Neural Networks (ANNs) outperform traditional models in accuracy. Moreover, the precision of predictions is contingent upon the combination of input parameters and the training algorithm employed (Barhoumi *et al*. 2017). A ground-breaking method for solar irradiance prognostication harnessing artificial neural networks is expounded, wherein the framework prognosticates three meteorological parameters employing metrics such as sunshine ratio, day number, and geographical coordinates (Che *et al*. 2018). Artificial neural networks constitute the cornerstone for devising solar irradiance prognostication frameworks, yielding outcomes showcasing a noteworthy alignment between computed and anticipated values (Crivellari and Beinat, 2020). Comparative scrutiny between Long Short-Term Memory (LSTM) neural networks and moving averages intimates the feasibility of the former for abbreviated solar energy forecasts (Eapen *et al*. 2019). Relative to alternative models, a simulation endeavour illustrates the pre-eminence of the LSTM model, showcasing data diminution via PCA as a means to truncate model training duration and augment its generalization aptitude (Fischer and Krauss, 2018). The real-time computation of solar radiation on inclined surfaces with diverse orientations engaged an Artificial Neural Network (ANN). The architecture of the ANN was honed and authenticated utilizing data drawn from the Klein and Theilacker model, in conjunction with comprehensive measurements (Gouda *et al*. 2016). Evaluation outcomes underscore the efficacy of profound networks in energy generation prognostication, with LSTM networks leveraged to delineate the interconnections amid various meteorological constituents and PV energy metrics (Hao and Gao, 2020). The essence of this endeavour hinges on formulating a straightforward solar irradiance prediction framework employing an advanced learning method, specifically Long Short-Term Memory (LSTM), leveraging solely cloud cover data procured from the National Meteorological Forecast Center (Husain *et al*. 2019). This investigation seeks to discern the

implications of utilizing multivariate data in solar radiation prediction through advanced learning techniques, proposing a multivariate forecasting model merging various meteorological factors, including temperature, humidity, and cloud cover (Liu *et al.* 2017).

The investigation confirms the viability of the proposed LSTM methodology in producing dependable Global Solar Radiation (GSR) forecasts. This validates the practical applicability of LSTM in renewable energy analyses and, more broadly, in energy monitoring instruments tailored for various energy parameters (Long *et al.* 2019). A sophisticated Deep Long Short-Term Memory (Deep LSTM) learning framework is recommended to address the smoothed monthly sunspot number (SSN), aiming to rectify the issue where prediction outcomes of current sunspot forecasting techniques lack consistency and display significant deviations (Makridakis *et al.* 2020). Employing an LSTM network, hourly solar irradiance forecasting for Johannesburg city is conducted utilizing a decade's worth of historical meteorological data sourced from Meteoblue (Pushparajesh *et al.* 2019). The efficacy of RNN and LSTM architectures, as measured by accuracy, is assessed using data from a 500 kW grid-connected plant (Smyl *et al.* 2023). The impact of LSTM on CNN-LSTM (Convolutional Neural Network-LSTM) performance concerning image fidelity is examined, showcasing its potential utility in image classification endeavors (Wang *et al.* 2018).

2. METHODOLOGY

In this article, the dataset is used for the prediction of theta which is the position of the solar panel. In this work, a standard 3 x 4 size rectangular solar panel is used. The solar panel position is tabulated concerning flux linkage at different radiation and temperature levels. The theta of the circular motion of structure arms is estimated using a regression model and fuzzy logic controller. The dataset consists of theta values for six different radiation and temperature levels for solar radiation (1.5, 5, 10, 15, 20, and 25 A). The fuzzy logic controller is designed in such a way that it will predict the theta using a regression model and this estimated theta is compared with the actual value. The attained error ranges from 0.1 to 0.9. The objective of this proposed method is to reduce this error further using the LSTM neural network. To train the LSTM model, one has to require a huge dataset. For that purpose, a regression model with a higher-order equation is used to extrapolate the dataset used. The actual dataset consists of 40 theta values for different radiation and temperature. The regression model undergoes training with this dataset across various polynomial orders. Simulation outcomes indicate that a polynomial order of 10 suffices to precisely replicate the actual dataset. Fig. 1 illustrates the juxtaposition between the actual and predicted datasets. The polynomial coefficient values are listed in Table 1.
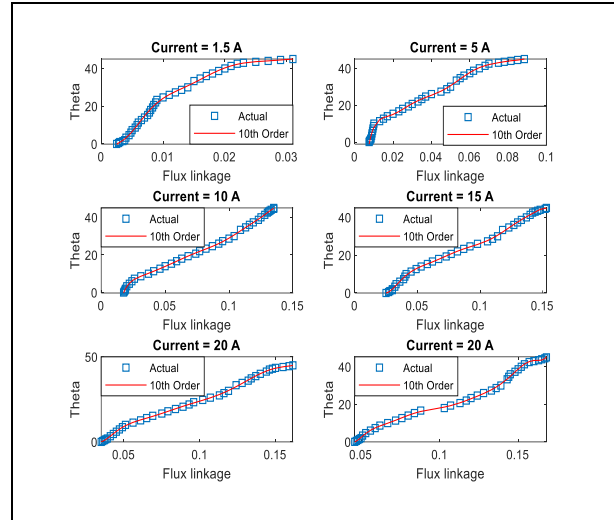

Fig. 1: Comparison of the actual data with the predicted data using a Regression model

Table 1. Regression model co-efficient at different radiation and temperature value

Radiation and temperature in Amps	10th order Co-efficient
1.5	[-0.15, 1.19, -2.78, -0.45, 10.55, -10.12, -9.20, 15.52, -4.49, 12.49, 27.68]
5	[0.43, -0.20, -8.25, 18.53, 3.45, -34.33, 7.94, 20.57, -3.13, 10.42, 24.29]
10	[-2.10, 0.26, 9.02, 1.47, -15.34, -5.90, 12.30, 6.83, -2.28, 11.33, 21.68]
15	[-1.40, -1.18, 10.79, 3.22, -26.15, -2.57, 23.42, 4.17, -6.29, 10.60, 22.93]
20	[0.29, -1.52, 1.76, 5.21, 10.29, -5.87, 12.39, 5.01, -2.44, 11.66, 22.18]
25	[6.50, 4.88, -29.90, -19.43, 45.82, 22.21, -28.52, -2.55, 11.08, 10.01, 19.57]

Using the polynomial coefficient from the Table 1, a linear equation is formed and 500 samples are generated. These datasets are used for training and validation purposes for the LSTM model. Machine learning is useful for two purposes namely regression and classification. In the classification model, a set of data is fed to the network for training purposes, and an unknown dataset is given to the network to check the performance of the model. In the realm of regression modeling, a predefined dataset of temporally dependent data is harnessed for training purposes, while the mean square error serves as the benchmark for assessing model performance. Here, the regression model is employed to

gauge the efficacy of the LSTM model. This study encompasses the utilization of three distinct model variants: LSTM, Bi-LSTM, and Deep LSTM.
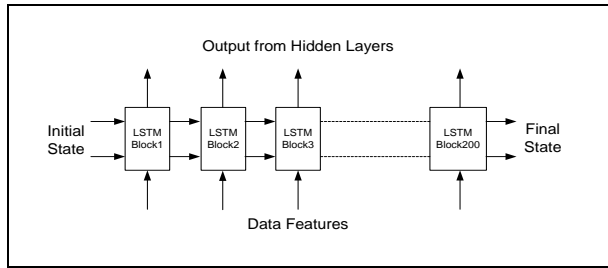

Fig. 2: Representation of LSTM architecture in the prediction process of solar panel position of Switched reluctance circular motion of structure arms
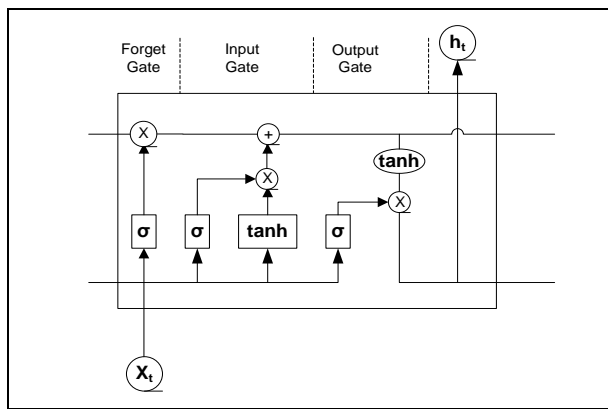

Fig. 3: Working flow diagram of a single cell in the LSTM network

LSTM network consists of several blocks connected in series form termed as cells or blocks. Sometimes cells are also referred as memory blocks as they can store the radiation and temperature state value. From one cell to another subsequent cell, two information will be shared known as the hidden state and cell state. Fig. 2 depicts the schematic portrayal of the LSTM network elucidated within this article. The operational intricacies of each memory block within the LSTM network shall be expounded upon, utilizing four distinct gates: the forget gate, input gate, and output gate, as illustrated in Fig. 3. As soon as the state of previous cell is received by the radiation and temperature LSTM cell, forget gate will make sure that the information which is coming is useful for the prediction purpose or not. If it is required then it will hold the radiation and temperature state otherwise it will be discarded. This operation will be executed using the sigmoid and multiplier functions. It will also help optimize the performance of the LSTM network.
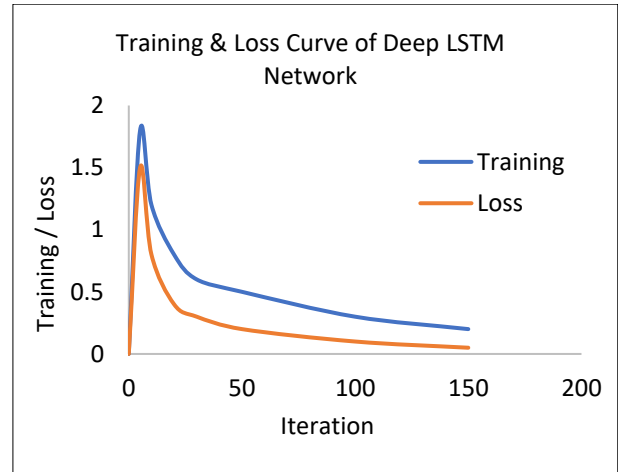

Fig. 4: Training curve, Loss curve of Deep LSTM network

Adding necessary information to the cell state will be done with the help of the input gate. It regulates the previous state value using sigmoid function and creates all possible vector values using 'tan h' function and finally, it will be added via the addition function. The input gate is also responsible in maintaining the non-repeatability of data. Output gate is the final gate in the LSTM network and its functionality will be brought down into three steps. The scaling of possible vectors from the input gate is normalized between -1 and +1 using 'tan h' function. Using the sigmoid function, the flow of data is regularized. This regulated output will also be sent to the hidden layer for further analysis.

Table 2. Comparison of RMSE at 80:20 training and testing ratio for subsequent sequence

Signal	Bi-LSTM		LSTM		Deep LSTM	
	Normal mode	**Predict & Update mode**	**Normal mode**	**Predict & Update mode**	**Normal mode**	**Predict & Update mode**
1 (I = 1.5 A)	2.3600	0.5294	4.7762	0.2048	2.0792	0.7551
2 (I = 5 A)	15.3693	3.5878	0.6137	0.1941	2.1195	0.8139
3 (I = 10 A)	29.7664	15.9441	3.854	0.5016	4.0818	3.5698
4 (I = 15 A)	4.0266	3.8324	4.1812	1.4934	3.2003	1.7064
5 (I = 20 A)	4.1868	4.1363	3.3821	1.5631	2.0004	1.9753
6 (I = 25 A)	20.5349	15.5049	5.9487	1.9944	3.0244	3.0213

Within the proposed framework, the theta value is designated as the network's response, while the flux linkage serves as its characteristic feature. The LSTM network incorporates a total of 200 hidden layers. To facilitate model training, an initial learning rate of 0.005 and a maximum epoch limit of 150 are employed for simulation purposes. The dataset is partitioned in a 90:10 ratio for training and validation, with 400 samples allocated for training and the remaining 100 samples earmarked for assessing the proposed model's performance. The training set with a one-time step delay is considered as the response or prediction of data. Table 2 shows the comparison of RMSE of types of LSTM networks to predict theta of the solar radiation.

LSTM network is operated in two different states: the first one is the normal mode, and the other one is the predict and update mode. In the normal mode, LSTM predicts the next state theta without considering the previous state output; whereas, in the predict and update mode, data is updated with the observed values at a particular instant rather than the predicted values. It is evident from Table 2 that the RMSE decreased a lot when the data are updated using predict one rather than in normal mode. To enhance the performance of the network, the training data is decimated by a factor of 2.

Table 3: Comparison of RMSE at 80:20 training and testing ratio with delayed sequence

Signal	Bi-LSTM		LSTM		Deep LSTM	
	Normal mode	Predict & Update mode	Normal mode	Predict & Update mode	Normal mode	Predict & Update mode
1 (I = 1.5 A)	27.7953	1.6029	1.5333	0.2145	1.2386	1.2531
2 (I = 5 A)	2.2563	2.3333	0.9093	0.2152	1.6349	0.8629
3 (I = 10 A)	6.9151	7.0118	2.2443	0.5214	1.2755	1.2733
4 (I = 15 A)	5.2539	5.3716	4.0724	1.3582	3.5239	1.6305
5 (I = 20 A)	4.1568	4.2176	1.7945	0.7335	1.1062	1.1139
6 (I = 25 A)	5.0823	4.4379	1.7738	0.6605	0.7871	0.6695

Table 4. Comparison of RMSE at 90:10 training and testing ratio for subsequent sequence

Signal	Bi-LSTM		LSTM		Deep LSTM	
	Normal mode	Predict & Update mode	Normal mode	Predict & Update mode	Normal mode	Predict & Update mode
1 (I = 1.5 A)	2.8932	1.7125	0.7568	0.1159	2.1908	0.9468
2 (I = 5 A)	13.943	3.1198	1.5567	0.5725	1.6372	2.1962
3 (I = 10 A)	20.0376	4.5280	2.1331	0.4196	6.6465	4.9856
4 (I = 15 A)	4.4941	0.9812	0.3958	0.1341	5.2753	2.8744
5 (I = 20 A)	18.7602	3.1510	2.8785	0.8799	2.5757	0.9766
6 (I = 25 A)	17.7819	2.6394	0.8531	0.1156	8.0966	8.0974

Table 5. Comparison of RMSE at 90:10 training and testing ratio with delayed sequence

Signal	Bi-LSTM		LSTM		Deep LSTM	
	Normal mode	Predict & Update mode	Normal mode	Predict & Update mode	Normal mode	Predict & Update mode
1 (I = 1.5 A)	3.9068	0.8808	0.1472	0.025	1.1046	1.2265
2 (I = 5 A)	4.6773	1.0192	0.7234	0.2643	5.3919	5.4491
3 (I = 10 A)	8.6824	5.3979	1.6972	0.7168	5.7033	4.9653
4 (I = 15 A)	6.9394	2.0953	0.1446	0.0642	5.9456	5.8103
5 (I = 20 A)	14.0125	2.5758	0.6484	0.0788	1.0772	1.2944
6 (I = 25 A)	14.9444	0.6279	2.8583	0.5349	5.491	5.8039

Table 3 shows the RMSE value of the LSTM network in the process of prediction of the solar radiation theta value. It is observed that significant result is achieved in terms of RSME of the Bi-LSTM and LSTM network. For the Deep LSTM network, the RMSE value is increased. Hence, the Deep LSTM network will not give better results when the data are not decimated. The above procedure is repeated for the training validation dataset in the ratio of 90:10. The results are presented in Tables 4 and 5. By observing the results from Tables 2 to 5, it is concluded that the performance of the LSTM network is better if more training datasets are involved. Figures 4 and 5 show the training curve, loss curve, and comparison of the actual with the predicted dataset using deep LSTM and LSTM network; a comparison of the actual phase angle with the predicted one was shown. It is evident that the LSTM network predicts the phase angle 100 percent compared to the Deep LSTM network.
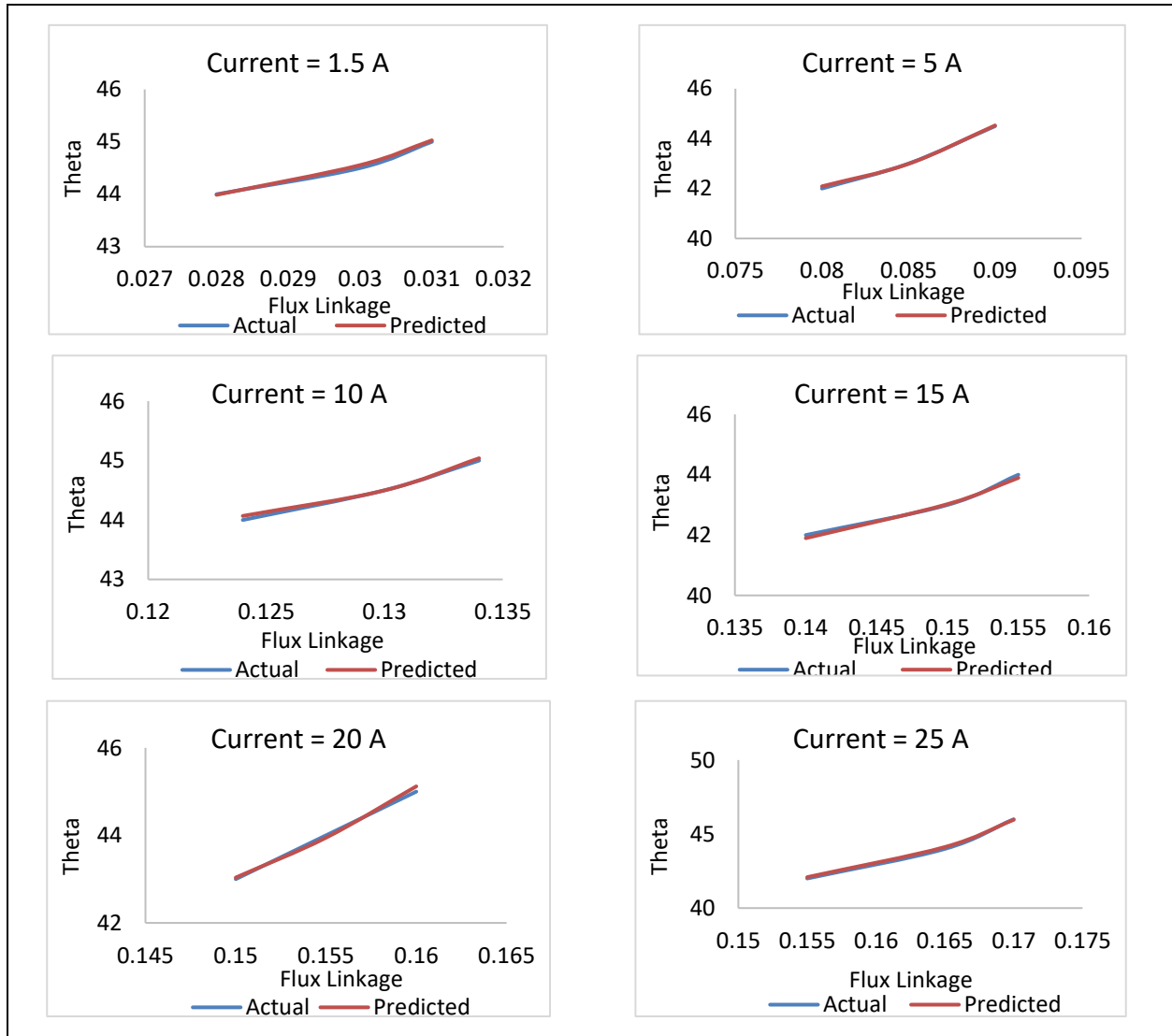

Fig. 5: Comparison of actual with predicted data using Deep LSTM network

4. RESULTS AND DISCUSSION

To analyze the performance of different types of LSTM networks in the prediction of the phase angle of solar radiation, RMSE value and percentile decrease in the RMSE value have been determined and shown in Figures 4 to 6. As the 80:20 training-testing ratio dataset is not providing good results, the 90:10 ratio dataset was considered and discussion was carried out accordingly. Figures 6 and 7 show the RMSE value with and without updation of data in the LSTM network. During the validation process, the LSTM network estimated phase angle values can be determined, whether by using the previously estimated or the present value alone. Accordingly, they are termed as with and without updated datasets. LSTM shows prominent results with

the least error value ranging from 0.3 to 2.8 for different values of radiation and temperature. The same LSTM network RMSE value ranges from 0.15 to 2.8 with the decimated input dataset; on the other hand, Bi-LSTM results in the worst RMSE value ranging from 2.8 to 20 for the actual dataset and 3.9 to 15 for the decimated dataset. Deep LSTM gives moderate RMSE between LSTM and Bi-LSTM.

Fig. 7 illustrates the RSME value of the LSTM network in the solar radiation phase angle prediction. In this case, the phase angle is predicted not only with the present value but also with the previous data with a one-time delay. RMSE value of the LSTM network ranges from 0.02 to 0.71 and 0.11 to 0.88 for decimated and un-decimated datasets respectively. Deep LSTM performs least compared to the other two types and its RMSE ranges from 1.22 to 5.8 and 0.9 to 8.09 with and without decimated datasets for different radiation and temperature values. Using the data result from Figures 4 and 5, the percentage decrease in the RMSE value is computed and shown in Fig. 8. The RMSE percentile decrease is another parameter to analyze the performance of the networks. All three types of LSTM show that there is a significant decrease in the RMSE value when the delay predicted data needs to be considered along with the present predicted values.
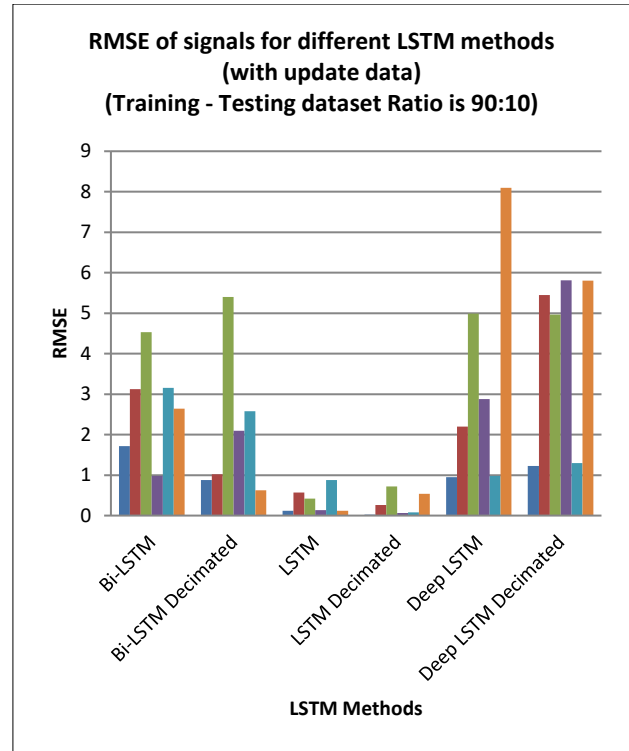

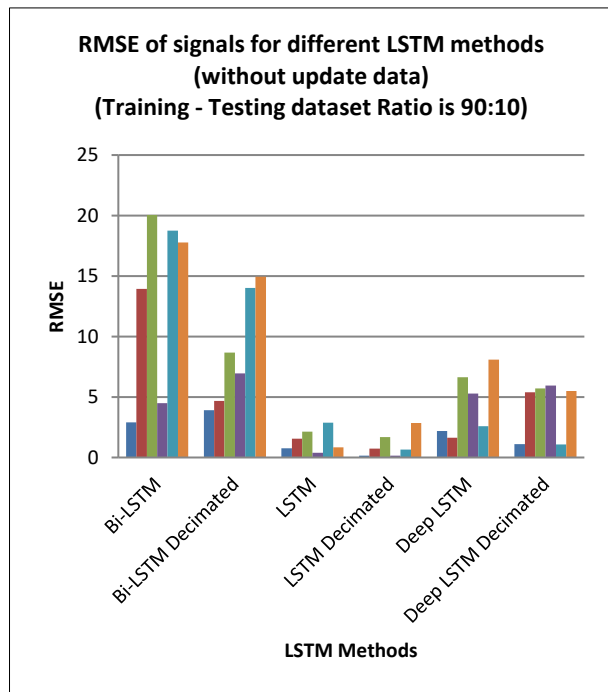Fig. 7: RMSE in the prediction of solar radiation theta value with data update

Fig. 6: RMSE in the prediction of solar radiation theta value without data update
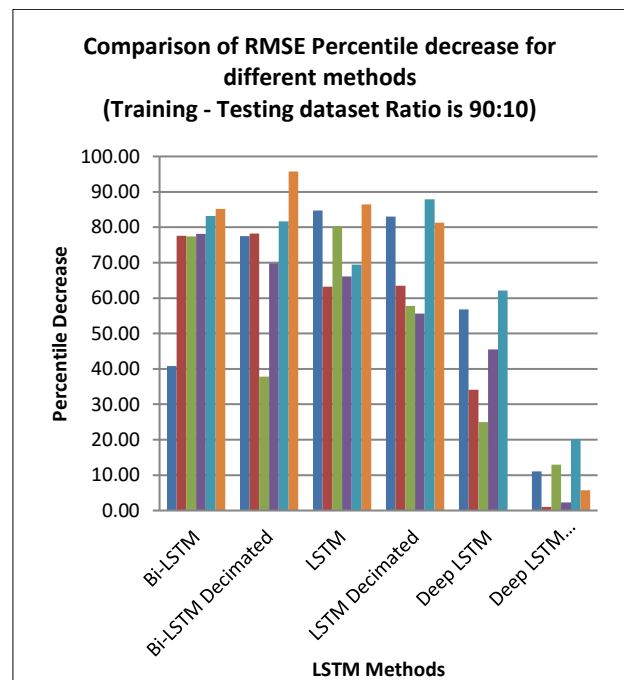

Fig. 8: Comparison of RMSE value with and without data update

5. CONCLUSION

LSTM network is a type of RNN network and it is trained to predict the solar radiation depending on solar panel position. Initially, a regression model with a polynomial order of 10 was used to generate from a few sample datasets. The dataset is trained by the network with two different categories. In the first method, the dataset was fed to the network without any decimation, and in the second method, the dataset was decimated by a factor of 2. The result concludes that the RMSE of the LSTM network gives promising results. During the prediction of the radiation and temperature forecast dataset, the trained sample between present and previous values was taken into consideration. It is termed as an updated LSTM value, A Comparison of the RMSE obtained by the LSTM and updated LSTM was carried out. It is evident from this comparison that the prediction of the theta value for the updated LSTM network was better than the normal LSTM. The researchers can extend this work by incorporating the hybrid CNN with the extracted feature of the dataset.

FUNDING

There is no funding source.

CONFLICT OF INTEREST

The authors declared no conflict of interest in this manuscript regarding publication.

COPYRIGHT

REFERENCES

Bao, W., A deep learning framework for financial time series using stacked autoencoders and long-short term memory, *PLOS ONE*, 12(7), e0180944(2017). https://doi.org/10.1371/journal.pone.0180944

Barhoumi, E.M., Abo-Khalil, A.G., Berrouche, Y. and Wurtz, F., Analysis and comparison of end effects in linear switched reluctance and hybrid motors, *J Electr Eng*, 68(2), 138–142(2017). https://doi.org/10.1515/jee-2017-0019

Che, Z., Purushotham, S., Cho, K., Sontag, D. and Liu, Y., Recurrent Neural Networks for Multivariate Time Series with Missing Values, *Sci. Rep.*, 8(1), 6085(2018). https://doi.org/10.1038/s41598-018-24271-9

Crivellari, A. and Beinat, E., LSTM-Based Deep Learning Model for Predicting Individual Mobility Traces of Short-Term Foreign Tourists, *Sustainability*, 12(1), 349(2020). https://doi.org/10.3390/su12010349

Eapen, J., Bein, D. and Verma, A., Novel Deep Learning Model with CNN and Bi-Directional LSTM for Improved Stock Market Index Prediction,. In: 2019 IEEE 9th Annual Computing and Communication Workshop and Conference (CCWC). IEEE, Las Vegas, NV, USA, 0264–0270 (2019). https://doi.org/10.1109/CCWC.2019.8666592

Fischer, T. and Krauss, C., Deep learning with long short-term memory networks for financial market predictions, *Eur. J. Oper. Res.*, 270(2), 654–669(2018). https://doi.org/10.1016/j.ejor.2017.11.054

Gouda, E., Hamouda, M. and Amin, A. R. A., Artificial intelligence based torque ripple minimization of Switched Reluctance Motor drives,. In: 2016 Eighteenth International Middle East Power Systems Conference (MEPCON). IEEE, Cairo, Egypt, 943–948 (2016). https://doi.org/10.1109/MEPCON.2016.7837010

Hao, Y. and Gao, Q., Predicting the Trend of Stock Market Index Using the Hybrid Neural Network Based on Multiple Time Scale Feature Learning, *Appl. Sci.*, 10(11), 3961(2020). https://doi.org/10.3390/app10113961

Husain, T., Elrayyah, A., Sozer, Y. and Husain, I., Unified Control for Switched Reluctance Motors for Wide Speed Operation, *IEEE Trans. Ind. Electron.*, 66(5), 3401–3411(2019). https://doi.org/10.1109/TIE.2018.2849993

Liu, S., Zhang, C. and Ma, J., CNN-LSTM Neural Network Model for Quantitative Strategy Analysis in Stock Markets,. In: Liu D, Xie S, Li Y, Zhao D, El-Alfy E-SM (eds) Neural Information Processing, Springer International Publishing, *Cham*, 198–206 (2017). https://doi.org/10.1007/978-3-319-70096-0_21

Long, W., Lu, Z. and Cui, L., Deep learning-based feature engineering for stock price movement prediction, *Knowl-Based Syst.*, 164163–173(2019). https://doi.org/10.1016/j.knosys.2018.10.034

Makridakis, S., Spiliotis, E. and Assimakopoulos, V., The M4 Competition: 100,000 time series and 61 forecasting methods, *Int. J. Forecast*, 36(1), 54–74(2020). https://doi.org/10.1016/j.ijforecast.2019.04.014

Pushparajesh, V., Balamurugan, M. and Ramaiah, N. S., Artificial Neural Network Based Direct Torque Control of Four Phase Switched Reluctance Motor,. *SSRN Electron. J.*, 1-8 (2019). https://doi.org/10.2139/ssrn.3371369

Smyl, S., Dudek, G. and Pełka, P., Contextually Enhanced ES-dRNN with Dynamic Attention for Short-Term Load Forecasting, *Electronic*, 1-11 (2023). https://doi.org/10.2139/ssrn.4331178

Wang, Y., Zhang, C., Wang, S., Yu, P. S., Bai, L. and Cui, L., Deep Co-Investment Network Learning for Financial Assets,. In: 2018 IEEE International Conference on Big Knowledge (ICBK), *IEEE, Singapore*, 41–48 (2018). https://doi.org/10.1109/ICBK.2018.00014